JACS
JOURNAL OF THE AMERICAN CHEMICAL SOCIETY
Article
pubs.acs.org/JACS

Substituent Effects on the [N−I−N]$^+$ Halogen Bond

Anna-Carin C. Carlsson,[†,∥] Krenare Mehmeti,[†] Martin Uhrbom,[†,▽] Alavi Karim,[†] Michele Bedin,[†,⊥] Rakesh Puttreddy,[§] Roland Kleinmaier,[†,¶] Alexei A. Neverov,[‡,⊗] Bijan Nekoueishahraki,[†] Jürgen Gräfenstein,[†] Kari Rissanen,[§] and Máté Erdélyi*[,†,#]

[†]Department of Chemistry and Molecular Biology, University of Gothenburg, SE-412 96 Gothenburg, Sweden
[‡]Department of Chemistry, Queen's University, Kingston, Ontario K7L 3N6, Canada
[§]Department of Chemistry, Nanoscience Center, University of Jyvaskyla, P.O. Box 35, Jyvaskyla FI-40014, Finland
[#]The Swedish NMR Centre, Medicinaregatan 5, SE-413 90 Gothenburg, Sweden

Supporting Information

ABSTRACT: We have investigated the influence of electron density on the three-center [N−I−N]$^+$ halogen bond. A series of [bis(pyridine)iodine]$^+$ and [1,2-bis((pyridine-2-ylethynyl)benzene)-iodine]$^+$ BF_4^- complexes substituted with electron withdrawing and donating functionalities in the *para*-position of their pyridine nitrogen were synthesized and studied by spectroscopic and computational methods. The systematic change of electron density of the pyridine nitrogens upon alteration of the *para*-substituent (NO_2, CF_3, H, F, Me, OMe, NMe_2) was confirmed by ^{15}N NMR and by computation of the natural atomic population and the π electron population of the nitrogen atoms. Formation of the [N−I−N]$^+$ halogen bond resulted in >100 ppm ^{15}N NMR coordination shifts. Substituent effects on the ^{15}N NMR chemical shift are governed by the π population rather than the total electron population at the nitrogens. Isotopic perturbation of equilibrium NMR studies along with computation on the DFT level indicate that all studied systems possess static, symmetric [N−I−N]$^+$ halogen bonds, independent of their electron density. This was further confirmed by single crystal X-ray diffraction data of 4-substituted [bis(pyridine)iodine]$^+$ complexes. An increased electron density of the halogen bond acceptor stabilizes the [N···I···N]$^+$ bond, whereas electron deficiency reduces the stability of the complexes, as demonstrated by UV-kinetics and computation. In contrast, the N−I bond length is virtually unaffected by changes of the electron density. The understanding of electronic effects on the [N−X−N]$^+$ halogen bond is expected to provide a useful handle for the modulation of the reactivity of [bis(pyridine)halogen]$^+$-type synthetic reagents.

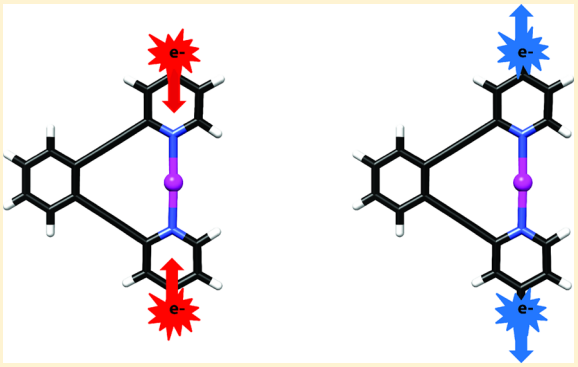

INTRODUCTION

A halogen bond (XB) is the close to linear, noncovalent interaction between an electron poor region of a halogen and an electron donor.[1] The chemical nature of the interaction was first rationalized by introduction of the σ-hole concept,[2] followed by description of the impact of charge-transfer, dispersion, polarization, and electrostatic forces.[3−9] Over the past decade, halogen bonds have been increasingly applied in a variety of research disciplines including material sciences, crystal engineering, structural biology, anion recognition and transportation, medicinal chemistry, organic synthesis, and organocatalysis.[6,10−13] Halogen bonding was recently utilized in the development of ionic liquid crystals,[14] in multidentate anion receptors,[15−18] and in the enantioselective recognition of chiral anions.[19] It was demonstrated to be applicable as noncovalent activator in organocatalysis,[20] and as a new tool in drug discovery.[11,21] It found application in the development of luminescent[22,23] and phosphorescent[24] optoelectronics, and of functional materials.[25,26] Halogen bonding has the potential to become a chemical tool as widely applicable as hydrogen bonding.

[Bis(pyridine)halogen]$^+$ complexes and their substituted analogues encompass a reactive halogen(I) species that is stabilized by two electron donors in an [N−X−N]$^+$ halogen bond. Both bromine(I) and iodine(I) containing complexes are useful reagents in organic synthesis, for example for electrophilic halogenation of alkenes, alkynes and aromatics, and for oxidations.[27−41] In three-center-four-electron [N−X−N]$^+$ halogen bonds,[42,43] the halogen is stabilized by simultaneous coordination to two nitrogen electron donors. The three atoms of the [N−X−N]$^+$ system may either form a static, symmetric geometry, [N···X···N]$^+$, or two asymmetric structures in a rapid equilibrium, [N−X···N]$^+$ ⇄ [N···X−N]$^+$,[44,45] the latter being analogous to the tautomeric exchange typical of related [N−H−N]$^+$ complexes.[46] In the symmetric [N···X···N]$^+$ geometry, the halogen forms two equally long and strong N···X bonds,

Received: April 14, 2016
Published: June 6, 2016

DOI: 10.1021/jacs.6b03842
J. Am. Chem. Soc. 2016, 138, 9853−9863

and its motion between the two nitrogens is described by a single-well energy potential. In contrast, in the asymmetric, dynamic system, in each asymmetric isomer the halogen forms one shorter and stronger covalent N–X bond, and one longer and weaker N···X halogen bond. As the halogen jumps between the two nitrogens, its motion is described by a double-well energy potential.[42,45] The centrosymmetric $[N–X–N]^+$ halogen bonds are particularly strong,[42,43,45,47] their strength being similar to that of the halogen bond of the isoelectronic $[I–I–I]^-$.[48] We have previously shown that the $[N–I–N]^+$ halogen bonds of [bis(pyridine)iodine]$^+$ (**1a**, Figure 1) and [1,2-bis((pyridine-2-ylethynyl)benzene)iodine]$^+$ (**2a**) complexes are exceptionally strong, and that their geometry is static symmetric in solution,[45,49] independent of the nature of the counterion present.[50]

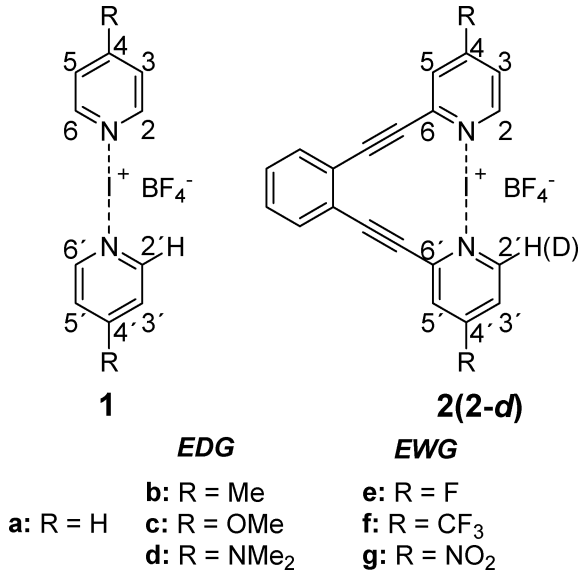

Figure 1. [Bis(4-R-pyridine)iodine]$^+$ BF_4^- (**1a–g**), and geometrically restrained [1,2-bis((4-R-pyridine-2-ylethynyl)benzene)iodine]$^+$ BF_4^- (**2a–g**) were used as model systems for evaluation of the influence of electron density alteration on the $[N–I–N]^+$ halogen bond. A systematic alteration of the electron density of the $[N–I–N]^+$ halogen bond was achieved by variation of the R-substituents, resulting in complexes with an increasing electron density in the order $NO_2 < CF_3 < H < F < Me < OMe < NMe_2$. Complex **1** permits free rotation and adjustment of N–I distances for the most favorable interaction, whereas the 1,2-diethynylbenzene backbone of **2** inhibits rotation around the N–I–N axis and imposes some strain in the N–I bonds to reach a geometrically optimal $[N–I–N]^+$ interaction. A mixture of **2a–d** and their monodeuterated isotopologs **2a–d-*d*** were used in IPE NMR experiments for determining the geometry of their $[N–I–N]^+$ halogen bonds.

The influence of electron density alteration on the strength and geometry of the three-center-four-electron $[N–X–N]^+$ halogen bond has so far not been assessed. A decreased electron donating ability of the nitrogens, as induced by electron withdrawing substituents, can be expected to destabilize the symmetric $[N–I–N]^+$ halogen bond, and increase the reactivity of the complex. If the central iodine(I) is unable to efficiently accept electrons into its empty p-orbital from two electron poor nitrogens simultaneously, it may prefer to compensate its electron depletion by forming a covalent bond to one of the nitrogens, instead of forming halogen bonds to both. Hence, electron depletion might induce an asymmetric $[N–I···N]^+$ geometry. In contrast, an increased electron density, induced by electron donating substituents, is expected to stabilize the symmetric $[N···I···N]^+$ geometry by strengthening the two N···I halogen bonds. This is expected to decrease the reactivity of the complex.

In this study, we report our findings, from systematic solution NMR, X-ray diffraction, reaction kinetics, and computational investigations on the influence of electron density alterations on $[N–I–N]^+$ halogen bond strength and geometry. An understanding of electronic effects is, above all, expected to provide a useful handle for the modulation of the reactivity of [bis(pyridine)halogen]$^+$-type reagents.

RESULTS AND DISCUSSION

[Bis(pyridine)halogen]$^+$ complexes and their geometrically restrained [1,2-bis((pyridin-2-ylethynyl)benzene)halogen]$^+$ analogues are the model systems typically used to gain understanding of the $[N–X–N]^+$ halogen bond.[42,43,45,49−51] In this study, we introduce substituents of varying electronic properties in the *para*-positions relative to the pyridine nitrogens (Figure 1), to study the influence of electron density alteration on the strength and geometry of their $[N–I–N]^+$ halogen bond.

Synthesis. The 4-substituted electron rich [bis(pyridine)-iodine]$^+$ BF_4^- complexes **1b** (4-Me), **1c** (4-OMe), and **1d** (4-NMe_2) as well as their electron poor analogue **1f** (4-CF_3), (Figure 1) were synthesized from their corresponding Ag^+ complexes by addition of molecular I_2, following our previously reported protocol[50] toward **1a**. Complex **1b** (4-Me) rapidly decomposed upon isolation.[52]

The 4-substituted [1,2-bis((pyridine-2-ylethynyl)benzene)-iodine]$^+$ BF_4^- complexes **2a** (4-H), **2b** (4-Me), **2c** (4-OMe), **2d** (4-NMe_2), **2e** (4-F), **2f** (4-CF_3), and **2g** (4-NO_2), and their selectively monodeuterated, electron rich analogues **2a–d-*d*** were prepared from their corresponding 1,2-bis(pyridine-2-ylethynyl)benzene ligands **3a** to **3g**, and **3b-*d*** to **3d-*d***, via their corresponding Ag^+ complexes,[50] as shown in Scheme 1. The electron poor $[N–I–N]^+$ complexes **2e** (4-F) and **2f** (4-CF_3) were observed by ^{1}H NMR to be significantly less stable in CD_2Cl_2 solution as compared to their electron rich analogues. Consequently, **2e** and **2f** could only be detected in a mixture with their decomposition product, the analogous $[N–H–N]^+$ complex. Our attempts to generate the electron poor complex **2g** (4-NO_2) yielded the corresponding $[N–H–N]^+$ complex only, due to the rapid decomposition of the targeted $[N–I–N]^+$ complex in solution.

The 4-substituted 1,2-bis(pyridine-2-ylethynyl)benzene ligands **3a–c,e,f** were synthesized using microwave-assisted Sonogashira coupling (Scheme 1),[53] following previously optimized conditions.[45] Compounds **3a** (4-H),[45] **3b** (4-Me),[54] and **3c** (4-OMe) were prepared from 1,2-diiodobenzene and two equivalents of terminal alkyne **4a–c**. Ligands **3e** (4-F) and **3f** (4-CF_3) were obtained from 1,2-diethynylbenzene and 2-bromo-4-fluoropyridine (**7e**) or 2-chloro-4-trifluoromethyl-py-ridine (**7f**).[54] The electron poor ligand **3g** (4-NO_2) was prepared from 1,2-diiodobenzene and 2 equiv of **4g** using Sonogashira coupling with Et_3N as base, instead of Et_2NH, and without microwave heating to avoid side reactions. The most electron rich ligand **3d** (4-NMe_2) was prepared from **3g** (Scheme 2) via Béchamp reduction,[55,56] followed by reductive amination of paraformaldehyde with sodium cyanoborohydride.[57]

DOI: 10.1021/jacs.6b03842
J. Am. Chem. Soc. 2016, 138, 9853−9863

Scheme 1. General Synthetic Route for the Synthesis of 4-Substituted [1,2-Bis((pyridine-2-ylethynyl)benzene)iodine]$^+$ BF_4^- Complexes 2a (4-H), 2b (4-Me), 2c (4-OMe), 2d (4-NMe_2), 2e (4-F), 2f (4-CF_3), and 2g (4-NO_2) and Their Selectively Monodeuterated Analogues 2a-d,g-*d*

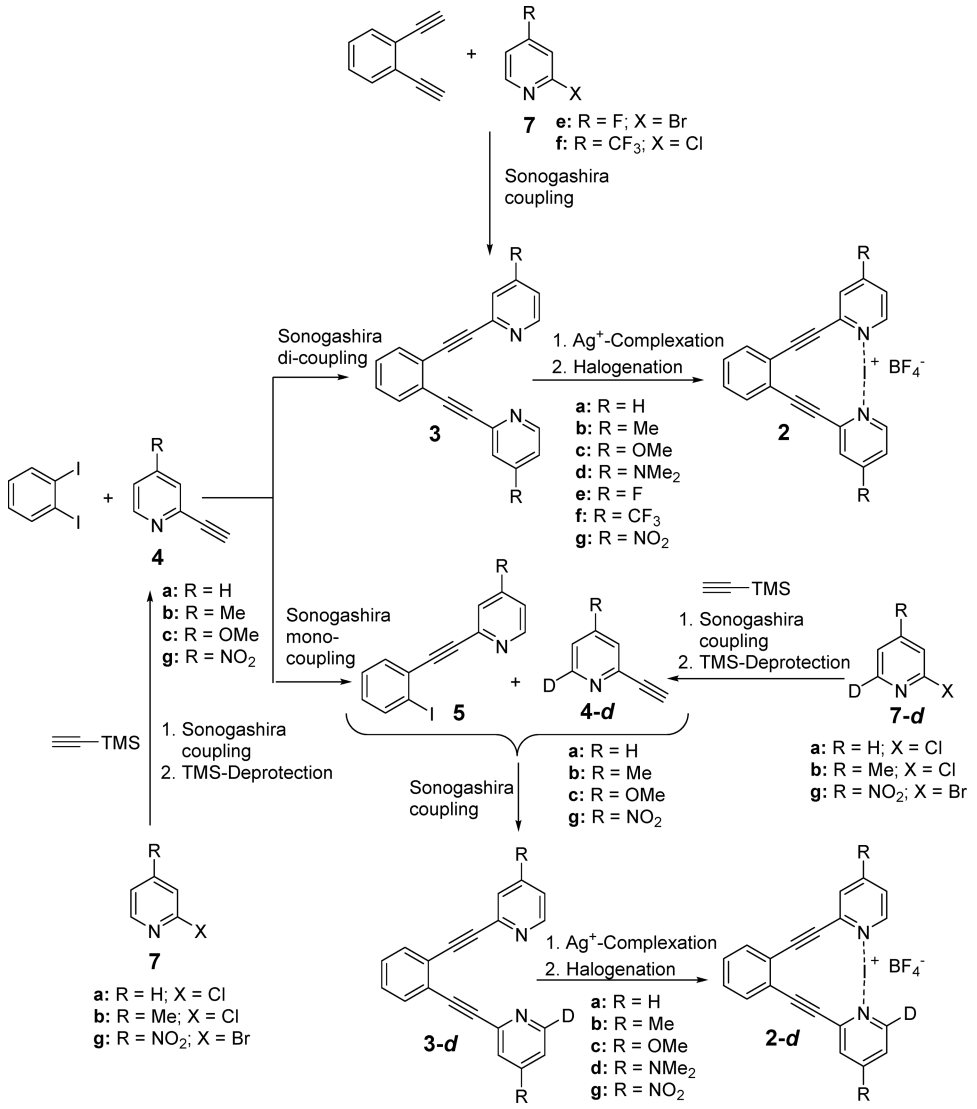

The monodeuterated ligands **3a-*d*** to **3c-*d*** were prepared in accordance with our reported procedure,[45] including two consecutive microwave-assisted Sonogashira couplings; coupling of 1,2-diiodobenzene with one equivalent of **4a−c**, generating **5a−c**, was followed by coupling of the corresponding deuterated terminal alkyne **4a-*d*** to **4c-*d*** (Scheme 1). The 4-NO_2-substituted analogue **3g-*d*** was prepared similarly from **5g** and **4g-*d***, and was then converted to the 4-NMe_2-subsituted **3d-*d*** via Béchamp reduction and subsequent reductive amination, as described above (Scheme 2) for the conversion of **3g** to **3d**. The terminal alkynes **4a-*d*** and **4b-*d*** were synthesized following our published procedure[45] via regioselective deuteration at C6 of either 2-chloropyridine (**7a**) or 2-chloro-4-methylpyridine (**7b**) using BuLi-LiDMAE, subsequent microwave mediated Sonogashira coupling of TMS-acetylene, and TMS-deprotection with KF in MeOH (Scheme 1).

The synthetic routes to the 4-MeO- and 4-NO_2-substituted terminal alkynes **4c** and **4g** (Scheme 3) both started from the commercially available 2-bromo-4-nitropyridine (**7g**), whereas those of their selectively monodeuterated analogues **4c-*d*** and **4g-*d*** started from 2-bromo-4-nitropyridine-6-*d* (**7g-*d***, Scheme 3). For selective monolithiation of 2,6-dibromopyridine at C-6 with *n*-BuLi, a method developed by Cai and co-workers was followed.[58] Successive electrophilic trapping with MeOD furnished 2-bromo-6-deuteropyridine (**8-*d***) in nearly quantitative yield. For introducing the 4-NO_2-group, **8-*d*** was first converted by *m*CPBA oxidation[59] into its *N*-oxide **9-*d***, which was then nitrated with H_2SO_4/HNO_3 to provide **10-*d***. Subsequent reduction of **10-*d*** with PBr_3 generated the desired starting material **7g-*d*** in high yield.[60] Sonogashira coupling of either **7g** or **7g-*d*** with TMS-acetylene at room temperature yielded the TMS-protected alkyne **6g** or **6g-*d***, following the procedure described by Sagitullina et al.[61] In subsequent TMS-deprotection, the 4-MeO- and 4-NO_2-substituted terminal alkynes **4c**/**4c-*d*** and **4g**/**4g-*d*** were selectively generated by the choice of reaction conditions. Deprotection with KF in MeOH at ambient temperature furnished 4-NO_2-substituted **4g**/**4g-*d***, whereas basic conditions using K_2CO_3 in THF/MeOH (1:1) at ambient temperature provided 4-MeO-substituted **4c**/**4c-*d*** as a result of simultaneous TMS-removal and nucleophilic replacement of the 4-NO_2-substituent. Further details regarding the

DOI: 10.1021/jacs.6b03842
J. Am. Chem. Soc. 2016, 138, 9853−9863

Scheme 2[a]

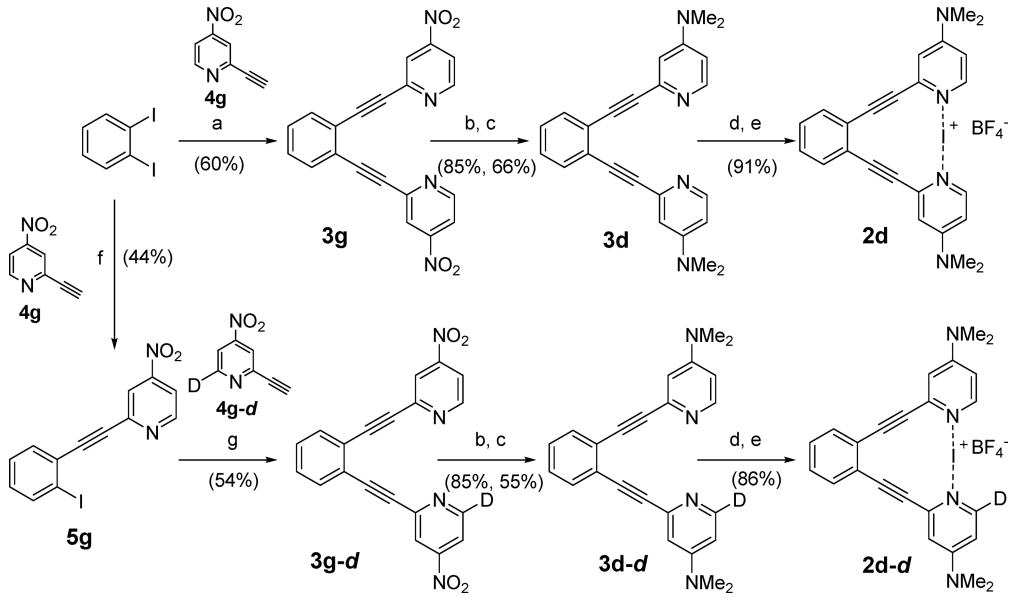

[a]Reagents and Conditions: (a) **4g** (2.2 equiv), $Pd(PPh_3)_2Cl_2$, CuI, Et_3N, 75 °C, 5 h, then rt, 18 h; (b) Fe, AcOH, 55 °C, 1.5 h; (c) CH_2O, $NaBH_3CN$, AcOH, rt, 24 h; (d) $AgBF_4$, CH_2Cl_2, rt, 20 min; (e) I_2, CH_2Cl_2, rt, 30 min; (f) **4g** (0.8 equiv), $Pd(PPh_3)_2Cl_2$, CuI, Et_3N, 75 °C, 3 h; (g) **4g-*d*** (2.1 equiv), $Pd(PPh_3)_2Cl_2$, CuI, Et_3N, 75 °C, 20 h.

Scheme 3[a]

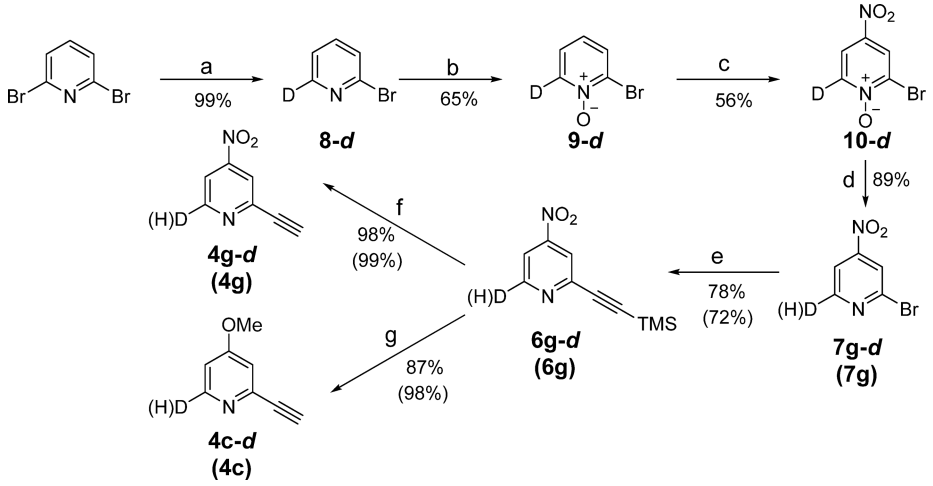

[a]Reagents and Conditions: (a) 1. *n*BuLi (1 equiv), THF, −78 °C; 2. MeOD (5 equiv), −78 °C, 1 h, then rt, 24 h; (b) *m*CPBA, $CHCl_3$, rt, 24 h; (c) HNO_3/H_2SO_4 2:1, 110 °C, 3 h; (d) PBr_3, CH_2Cl_2, 60 °C 3 h; (e) TMS-acetylene, $Pd(PPh_3)_2Cl_2$, CuI, Et_3N, 5 °C, 1 h, then rt, 2 h; (f) KF, MeOH, rt, 2 h; (g) K_2CO_3, THF/MeOH 1:1, rt, 1 h.

syntheses described above are given in the Supporting Information.

Alteration of Electron Density. A common approach to increase XB strength is to enhance the electrophilicity of the halogen bond donor using strongly electron withdrawing substituents.[62] Accordingly, perfluoroaryl and -alkyl halides are frequently applied halogen bond donors in model studies. The alternative approach is to increase the electron density of the halogen bond acceptor by the introduction of electron donating substituents.[63] A stronger halogen bond is often presumed to be reflected by a shorter distance between the halogen bond donor and the acceptor.[48,64,65] Computational studies revealed that the Hammett substituent constants of pyridine-based halogen bond acceptors correlate to the strength of their halogen bond.[66,67] Strategic tuning of halogen bond strength is expected to facilitate the development of halogen transfer reagents and of supramolecular systems,[12,20] for example.

The Hammett substituent constants, and the corresponding induction and resonance constants *F* and *R*, are reported for benzene derivatives and are not calibrated for pyridine rings. To assess how well they describe electron donation/withdrawal in pyridine rings, we calculated the natural atomic population (NAP[68]) n(N) as well as the π electron population n_π(N) for the nitrogen atoms of **1a**−**g** and **2a**−**g**. The calculations were performed with the computational protocol described below for the investigation of equilibrium geometries and bond energies. The changes of these populations, Δn(N) and Δn_π(N), relative

DOI: 10.1021/jacs.6b03842
J. Am. Chem. Soc. 2016, 138, 9853−9863

to **1a** and **2a**, respectively, are listed in Table 1, together with the corresponding Hammett and resonance constants.

Table 1. Calculated Changes Upon Substitution for Natural Atomic Populations Δn(N) and π Orbital Populations Δn_π(N) for the N atoms of Iodine(I) Complexes 1a−g and 2a−g, versus Hammett and Resonance Substituent Constants

structure	4-R	σ_{para}	$10^3 \times \Delta n$(N)	R	$10^3 \times \Delta n_\pi$(N)
1a	H	0	0	0	0
1b	Me	−0.17	3.0	−0.18	12.7
1c	OMe	−0.27	5.9	−0.56	42.6
1d	NMe_2	−0.83	18.5	−0.98	73.2
1e	F	0.06	−7.9	−0.39	16.7
1f	CF_3	0.54	−17.7	0.16	−15.5
1g	NO_2	0.78	−30.7	0.13	−25.9
2a	H	0	0	0	0
2b	Me	−0.17	2.7	−0.18	11.6
2c	OMe	−0.27	5.9	−0.56	39.8
2d	NMe_2	−0.83	17.1	−0.98	69.2
2e	F	0.06	−6.3	−0.39	16.9
2f	CF_3	0.54	−15.1	0.16	−11.4
2g	NO_2	0.78	−26.7	0.13	−19.1

Regression coefficients of 0.969 (**1a−g**) and 0.973 (**2a−g**) between σ_{para} and Δn(N), and 0.965 (**1a−g**) and 0.975 (**2a−g**) between R and Δn_π(N) are found. Thus, the correlations are indeed distinct, but not perfect. We therefore used Δn(N) and Δn_π(N) directly to quantify the electron withdrawing/donating properties of substituents.

The ^{15}N NMR chemical shift, δ^{15}N, is recognized to be a sensitive tool for the assessment of the coordinative bonds of nitrogen heterocycles.[54,69] It has previously been used for the characterization of halogen bonded complexes.[45,49,50,70,71] Upon formation of pyridine-based $[N\cdots I\cdots N]^+$ complexes, analogous to nonsubstituted **1a** and **2a**, ∼100 ppm ^{15}N chemical shift changes, $\delta^{15}N_{coord}$, are induced.[45] This chemical shift alteration is the consequence of the establishment of a strong halogen bond, in which the pyridine nitrogen acts as Lewis base, and the introduction of a positive charge into the molecular system. The bond strength of nitrogen heterocycles is commonly assessed by the ^{15}N NMR coordination shift, $\delta^{15}N_{coord}$. It is defined as the ^{15}N chemical shift difference of a complex and of its corresponding free nitrogen base (ligand), i.e., $\delta^{15}N_{coord} = \delta^{15}N_{complex} - \delta^{15}N_{ligand}$. A stronger coordinative bond is commonly seen to be reflected by a larger $|\delta^{15}N_{coord}|$.[45,49] To evaluate the influence of substituents on the electron density of the pyridine nitrogen involved in the formation of $[N\cdots I\cdots N]^+$ complexes, we acquired the ^{15}N NMR chemical shift for **1a−d,f** and **2a−f** (Figure 1), $\delta^{15}N_{complex}$, and for their corresponding free nitrogen bases (4-substituted pyridines and **3a−f**), $\delta^{15}N_{ligand}$. The δ^{15}N values were detected for CD_2Cl_2 solutions using indirect detection by ^{1}H,^{15}N HMBC experiments. A single ^{15}N NMR signal was observed for each complex (Table 2). Electron donating substituents in the *para*-position of the pyridine nitrogen increase the shielding of the nitrogen, whereas electron withdrawing substituents have an opposite effect. The influence of the substituents on the δ^{15}N is comparable for the ligands and complexes applied in this study. We determined the regression coefficients r^2 for the correlation of δ^{15}N with both Δn(N) and Δn_π(N), as well as σ_{para} and R, both for the series of complexes **1a−d,f** and **2a−f** and for the

Table 2. ^{15}N NMR Chemical Shift (ppm) of Iodine(I) Complexes 1a−d,f and 2a−f, and of the Corresponding Nitrogen Bases[a]

structure	4-R	$\delta\ ^{15}N_{complex}$	$\delta\ ^{15}N_{ligand}$	$\delta\ ^{15}N_{coord}$
1a	H	−175.1	−67.0	−108.1
1b	Me	−180.2	−71.6	−108.6
1c	OMe	−195.0	−86.0	−109.0
1d	NMe_2	−214.2	−104.8	−109.4
1f	CF_3	−164.1	−51.6	−112.5
2a	H	−165.5	−64.5	−101.0
2b	Me	−170.2	−69.2	−101.0
2c	OMe	−183.5	−83.5	−100.0
2d	NMe_2	−202.9	−102.2	−100.7
2e	F	−170.9	−69.5	−101.4
2f	CF_3	−156.7	−50.7	−106.0

[a]The ^{15}N NMR coordination shifts represent the chemical shift change upon complex formation.

corresponding series of ligands (see SI for the complete results). For the correlation with Δn_π(N), the r^2 values are in the interval between 0.984 (ligands for **1a−d,f**) and 0.995 (complexes **1a−d,f**) (Figure 2), whereas for the correlation

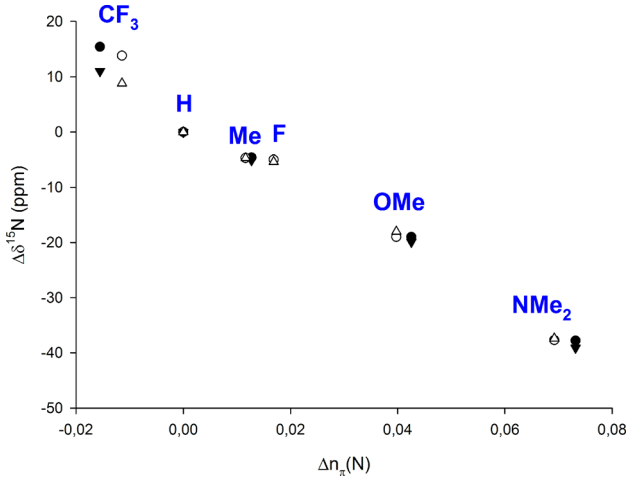

Figure 2. ^{15}N NMR chemical shift changes (relative to **1a** or **2a**, respectively), $\Delta\delta^{15}$N, of substituted pyridines (●), of the corresponding 1,2-bis((pyridine-2-ylethynyl)benzene) ligands **3a−f** (○), and of their $[N{-}I{-}N]^+$ complexes, **1a−d,f** (▼) and **2a−f** (Δ), respectively, strongly correlate to the corresponding changes in the π(N) orbital population. This indicates that the variation in δ^{15}N is dominatingly governed by the paramagnetic ring currents in the pyridine moieties.

with Δn(N) considerably lower r^2 values, in the interval between 0.824 (complexes **2a−f**) and 0.920 (ligands **3a−f**), were calculated. Likewise, the regression coefficients with respect to σ_{para} and R were lower than the r^2 with respect to Δn_π(N). This finding indicates that the substituent effects on the δ^{15}N are governed by the π population rather than the total electron population at the nitrogen atoms. Thus, the δ^{15}N is primarily controlled by the paramagnetic ring currents of the pyridine rings rather than by diamagnetic shielding or deshielding. Consequently, the δ^{15}N change is a specific measure for the π donating or withdrawing property of substituents. In particular, we find that fluorine, in contrast to common beliefs, dominantly acts as an electron donor, via resonance, which is reflected by the comparable δ^{15}N of the fluorine substituted **2e** and **3e** to those of the methyl

DOI: 10.1021/jacs.6b03842
J. Am. Chem. Soc. 2016, 138, 9853−9863

substituted analogues **2b** and **3b** (Table 2). This observation is corroborated by the literature.[72] The $\delta^{15}N_{coord}$ of the iodine(I) complexes do not vary to a significant extent, which is in excellent agreement with previous observations of $\delta^{15}N_{coord}$ for analogous silver(I) complexes, when detected in a non-coordinating solvent and in the absence of a strongly coordinating counterion.[50,54] Overall, the observed large $\delta^{15}N_{coord}$ of **1a−d,f** and **2a−f** confirms formation of $[N{-}I{-}N]^+$ complexes; however, its magnitude does not reflect interaction strength.

Halogen Bond Symmetry in Solution. Understanding the factors governing the geometry of the three-center-four-electron $[N{-}X{-}N]^+$ halogen bond is a key for the description of its nature.[42,43,45,51] The solution NMR spectroscopic technique isotopic perturbation of equilibrium (IPE) has previously been proven to be a unique tool for distinguishing a rapidly equilibrating mixture from a static, symmetric structure in solution, and was successfully applied for symmetry determinations of hydrogen and halogen bonds, of carbocations, and of metal chelates.[45,46,73,74] IPE relies on the detection of vibrational energy changes in a molecule upon selective isotope labeling, commonly a hydrogen to deuterium substitution close to the interaction site of interest. When analyzing the mixture of the labeled and the unlabeled isotopologs of a compound, two sets of signals are detected; one set originates from the nondeuterated compound, whereas the other set stems from the deuterated analogue. The small shift difference between the signals of the isotopologs is called the isotope shift, $^n\Delta_{obs}$, where n denotes the number of bonds between the observed nucleus, commonly ^{13}C, and the position of the isotopic substitution. The observed chemical shift difference is the sum of the intrinsic isotope shift, $^n\Delta_0$, and the equilibrium isotope shift, $^n\Delta_{eq}$, according to eq 1:

$$^n\Delta_{obs} = \delta_{C(D)} - \delta_{C(H)} = {}^n\Delta_0 + {}^n\Delta_{eq} \quad (1)$$

The intrinsic isotope effect, $^n\Delta_0$, which is present in all systems, is usually small and attenuates as n increases. The $^1\Delta_0$ and $^2\Delta_0$ isotope shifts, observed for the reporter atoms one and two bonds from the isotopic substitution site, are negative, often in the order of −0.3 ppm and −0.1 ppm, whereas the sign of $^n\Delta_0$ observed for reporter atoms further away may vary. The equilibrium isotope effect, $^n\Delta_{eq}$, in contrast, is present only for systems involved in a dynamic equilibrium process, and is zero for static systems. Its magnitude depends on the equilibrium constant K of the exchange process:

$$^n\Delta_{eq} = D(K-1)/[2(K+1)] \quad (2)$$

where D denotes the chemical shift difference between the signals of the isomeric forms, i.e., halogenated $N^+{-}X$ and nonhalogenated N, in this particular case. The equilibrium constant, K, is temperature dependent according to the van't Hoff equation,[75] and so is the equilibrium isotope effect, $^n\Delta_{eq}$. We have shown that the magnitude of the observed isotope shift, $^n\Delta_{obs}$, does not allow straightforward differentiation between a static $[N{\cdots}X{\cdots}N]^+$ geometry and a dynamic $[N{-}X{\cdots}N]^+ \rightleftarrows [N{\cdots}X{-}N]^+$ system in rapid equilibrium, but the temperature dependence of $^n\Delta_{obs}$ is a reliable measure for distinguishing the two systems from each other.[45] The symmetry of the $[N{-}I{-}N]^+$ halogen bond of **2a−d** was studied in solution with the IPE technique using isotopolog mixtures and ^{13}C $\{^1H,^2H\}$ NMR detection, as described in detail earlier.[45] Similar to previous studies of halogen bond symmetry,[45,49,50] isotopolog mixtures of the free ligands **3a−d** were used as references for static systems in the evaluation of the temperature dependence of the isotope effects (Table 3). Due to their low stability, in combination with their poor solubility, the symmetry of the electron poor complexes **3e−g** could not be studied experimentally.

Table 3. Temperature Coefficients (ppm × K) of the ^{13}C Isotope Shifts of Complexes 2a−d, and the Corresponding References 3a−d for a Static Geometry

structure	4-R	C2 $^1\Delta_{obs}$	C3 $^2\Delta_{obs}$	C4 $^3\Delta_{obs}$	C5 $^4\Delta_{obs}$	C6 $^3\Delta_{obs}$	$\Sigma\,\lvert\Delta_{obs}\rvert$
2a[a,c]	H	−8.9	−10.8	+0.7	0	−2.0	22.4
3a[a,d]	H	−8.1	−9.1	−1.5	+3.4	−4.5	26.6
2b[a]	Me	−11.2	−11.3	+1.3	0	−2.5	26.3
3b[b]	Me	−8.8	−8.6	n.d.[e]	+3.0	n.d.[e]	(20.4)
2c[b]	OMe	−5.4	−11.5	+2.3	0	−3.1	22.3
3c[b]	OMe	−5.9	−8.9	+2.3	0	0	17.1
2d[b]	NMe_2	−5.8	−10.2	+3.2	0	n.d.[e]	(19.2)
3d[b]	NMe_2	−4.1[c]	−9.2	+0.9	+1.1	−4.9	16.1

[a]The $^{13}C\{^1H,^2H\}$ experiments were run at 125.71 MHz. [b]The $^{13}C\{^1H,^2H\}$ experiments were run at 201.20 MHz. [c]Temperature interval −20 to 25 °C. [d]Temperature interval −10 to 25 °C. [e]Due to minor temperature dependence and to limited solubility, this coefficient could not be reliably determined.

The temperature coefficients $^n\Delta_{obs}$ for complexes **2a−d** (Table 3) are small and comparable to those of the corresponding reference molecules **3a−d**, in both magnitude and sign. The sum of the absolute value of the observed isotope effects, $\Sigma|\Delta_{obs}|$, is comparable for the free ligands and their corresponding $[N{-}I{-}N]^+$ halogen bonded complexes. The overall temperature dependence of the isotope effect of systems involved in rapid equilibrium, such as $[N{-}H{-}N]^+$ complexes, were previously reported to be significantly higher than those of their corresponding free ligands.[45] In agreement with previous studies,[45,49,50,76] the $^2\Delta_{obs}$'s of C3 were largest for both the free ligands **3a−d** and their iodine(I) complexes **2a−d**. A static, symmetric geometry of **2a−d**, independent of the electron density of their $[N{\cdots}I{\cdots}N]^+$ bond, was further indicated by the relative magnitude of the temperature coefficients. Thus, a larger temperature dependence was detected for the carbons closest to the position of ^1H-to-^2H substitution, $^1\Delta_{obs}$ and $^2\Delta_{obs}$. For dynamic systems, such as the corresponding $[N{-}H{-}N]^+$ complexes, the magnitude of the temperature coefficients depends not only on the distance of the reporter ^{13}C's to the deuterium substitution site (n), but also on their distance to the nitrogen that is directly involved in the fast equilibrium process.[45] Consequently, the temperature coefficients of the isotope effects of carbons further away from the point of isotope substitution, yet close to the nitrogen are large for dynamic, but small for static systems.

For a more detailed analysis of the halogen bonds and their symmetry, we calculated equilibrium geometries and energies of **1a−g** and **2a−g**. All calculations were performed using density functional theory (DFT), employing the B3LYP exchange and correlation functional.[77−79] The LANL08 basis set[80] in conjunction with LANL2DZ effective core potential[81−83] were used for I, whereas Pople's 6-311+G(d,p)[84−86] basis set was used for N, and Pople's 6-311G(d,p)[84,85] basis set for the remaining atoms. Solvent effects were accounted for by the Polarizable Continuum Model (PCM)[87,88] with dichloro-

DOI: 10.1021/jacs.6b03842
J. Am. Chem. Soc. 2016, 138, 9853−9863

methane as solvent. Calculations predict symmetric equilibrium geometries for compounds **1a–g** and **2a–g** (Table 4), with N–I distances that are 18% (~0.41 Å) longer than that of the corresponding N–I covalent bond (2.077–2.094 Å, Table S31, Supporting Information), and considerably shorter than the sum of the van der Waals radii of the participating atoms (3.53 Å, R_{XB}= 0.65[50,64,89]). The bond lengths for the geometrically restrained (**2**) and the corresponding nonrestrained analogues (**1**) differ by less than 0.01 Å, indicating that the strain energy required to distort the 1,2-ethynylbenzene backbone is small as compared to the energetic gain upon forming a symmetric three-center $[N–I–N]^+$ halogen bond.[45] Upon formation of the $[N–I–N]^+$ complexes **2a–f**, the N–N distance decreases by 0.07 to 0.2 Å, whereas for **2g**, it slightly increases by 0.007 Å. The N–I–N angle is linear (180°) for the [bis(pyridine)-iodine]$^+$ complexes **1a–g**, and is approximately 175.5° for the [1,2-bis((pyridine-2-ylethynyl)benzene)iodine]$^+$ complexes **2a–g**, in excellent agreement with previous reports on the geometry of halogen bonds.[6,10,42,48] The N–I bond length shows only minor dependence on the electronic properties of the substituent, with a less than 0.02 Å difference observed between the shortest and longest bonds. The N–I bond length correlates with the π electron population, Δn_π(N), with r^2 of 0.953 (**1a–g**) and 0.935 (**2a–g**), (Figure 3). Significantly lower correlation was found between r(N–I) and the total electron population Δn(N), as reflected by the r^2 0.800 for **1a–g**, and 0.700 for **2a–g**. This indicates that the slight variation in the N–I bond length of the studied complexes is governed by the π population at the nitrogen atoms. To assess the stability of complexes **1a–g** and **2a–g**, we calculated their stabilization energies according to the formal reactions shown in Scheme 4. Since we are interested in the strength of the electronic bond rather than wish to make a comparison to experimental thermochemical data, the electronic energies are considered here and not the Gibbs free energies. Whereas the geometry, i.e., the bond lengths and bond angles, of the complexes is virtually independent of electron density, their stability varies by nearly 100 kJ/mol, depending on the electronic nature of the substituents (Table 4, Figure 4). An increased electron density stabilizes the $[N\cdots I\cdots N]^+$ bond (**1b–d** and **2b–d**), whereas electron deficiency reduces the stability of the complexes (**1e–g** and **2e–g**). The correlation coefficients between the stabilization energy, ΔE_{stab}, and the natural atomic population, Δn(N), are 0.991 for **1a–g** and 0.989 for **2a–g**, whereas the corresponding r^2 values for the π electron population, Δn_π(N), are significantly lower, 0.851 for **1a–g**, and 0.828 for **2a–g**. Thus, whereas the N–I bond length proved to correlate strongly with Δn_π(N), the stabilization energy correlates nearly perfectly with the total natural atomic population (NAP) at the nitrogen atoms. This can be rationalized from the mechanism of the three-center-four-electron $[N\cdots I\cdots N]^+$ bond: the larger the natural atomic population, Δn(N), the higher the energies of the occupied orbitals at the nitrogen, which facilitates the charge transfer to iodine(I). This is in line with the findings of Ebrahimi et al., who investigated the nature of the $[N\cdots X\cdots N]^+$ bond with a variety of theoretical methods.[90] The computationally predicted variation of the $[N\cdots I\cdots N]^+$ bond strength agrees excellently with the experimentally observed higher stability of electron rich complexes **2b–d** as compared to the unsubstituted **2a**, and the instability of **2e** in solution that prevented their IPE study. It should be noted that the rapid decomposition of **2g** prevented its experimental investigation completely, in line with its computationally predicted instability.

We emphasize that the correlations found above must not be misinterpreted as causal relationships. For instance, the close correlation between Δn(N) and ΔE_{stab} does not indicate that the halogen bond strength is governed solely by electrostatic interactions between the partial charges of the N and I atoms. Rather, as has been discussed, e.g., in ref 10, halogen bonding is caused by an interplay between electrostatic, charge-transfer and not the least polarization and dispersion effects. The Δn(N) and Δn_π(N) values are to be considered just as indicators for the properties of the substituents, in lieu of properly calibrated Hammett, induction, and resonance constants.

Geometry in the Solid State. Single crystals were obtained via slow diffusion of hexane into dichloroethane solutions of **1c** and **1f** under cooling from 24 °C to −20 °C

Table 4. Computationally Predicted N–I and N–N Distances, N–I–N Angles, and Stabilization Energies for Complexes 1a–g and 2a–g and N–N Distances for the Ligands 3a–g[a]

structure	4-R	r(NI)[b] (Å)	r(NN)[c] (Å)	r(NN)[d] (Å)	∠(NIN) (deg)	ΔE_{stab} (kJ/mol)
1a	H	2.3036	4.6072		180	0
1b	Me	2.3013	4.6026		180	12.7
1c	OMe	2.2980	4.5960		180	42.6
1d	NMe_2	2.2921	4.5841		180	73.2
1e	F	2.3032	4.6063		180	16.7
1f	CF_3	2.3055	4.6109		180	−15.5
1g	NO_2	2.3065	4.6131		180	−25.9
2a	H	2.3034	4.5934	4.6854	175.7	0
2b	Me	2.3011	4.5875	4.7166	175.4	11.6
2c	OMe	2.2982	4.5832	4.6586	175.7	39.8
2d	NMe_2	2.2930	4.5715	4.7700	175.4	69.2
2e	F	2.3027	4.5921	4.6756	175.7	16.9
2f	CF_3	2.3041	4.5939	4.6624	175.5	−11.4
2g	NO_2	2.3043	4.5952	4.5880	175.7	−19.1

[a]All calculations were done for CH_2Cl_2 solution with the computational protocol described below. [b]For all compounds, $r(NI)_1 = r(NI)_2$. [c]$[N–I–N]^+$ complexes **1a–g** and **2a–g**. [d]Ligands **3a–g**.

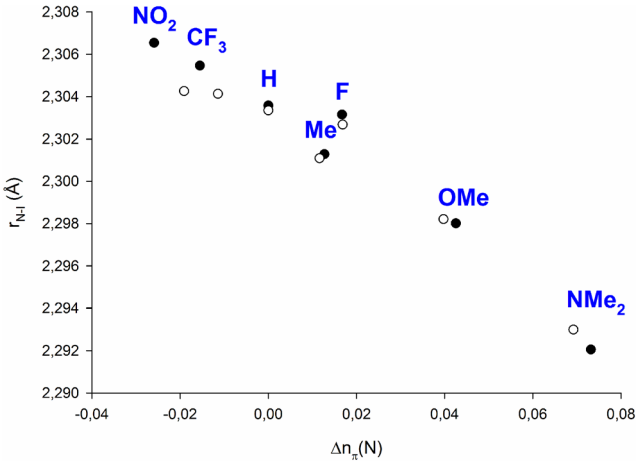

Figure 3. Correlation of the N–I bond distance with the change in the π(N) population of iodine(I) complexes of substituted pyridines (**1a–g**) (●) and of the corresponding 1,2-bis((pyridine-2-ylethynyl)-benzene) ligands (**2a–g**) (○).

DOI: 10.1021/jacs.6b03842
J. Am. Chem. Soc. 2016, 138, 9853–9863

Scheme 4. Formal Reactions Used to Define the Stabilization Energies of Complexes 1a–g and 2a–g

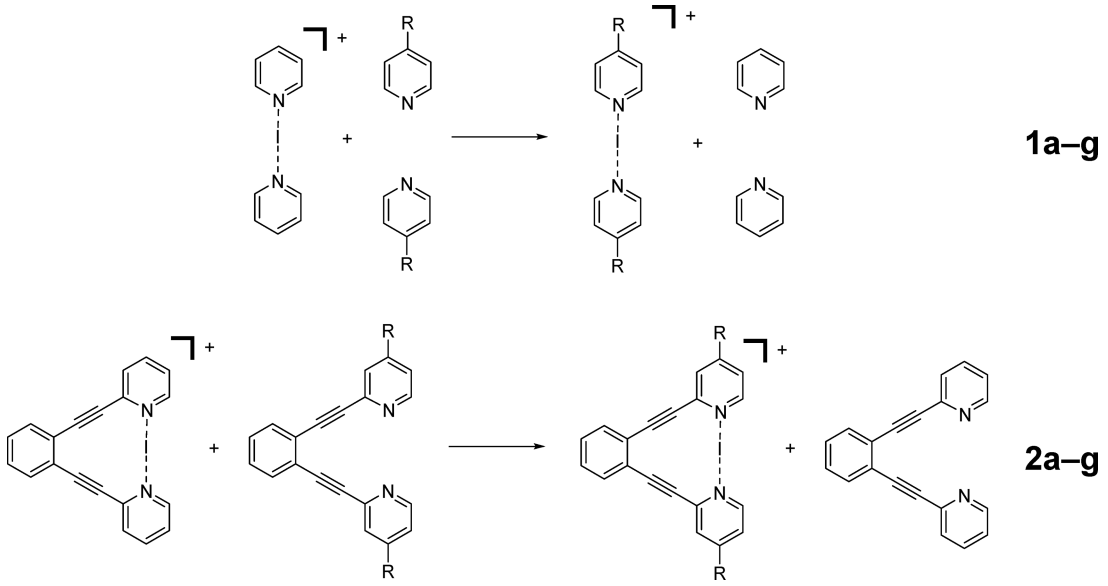

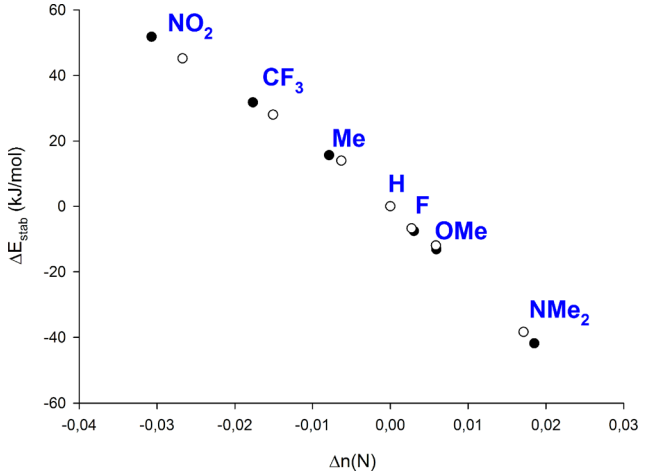

Figure 4. Correlation of the stabilization energy (ΔE_{stab}) and the change of the natural atom population at the N atoms of the iodine(I) complexes of substituted pyridines (**1a–g**) (○) and of the corresponding 1,2-bis((pyridine-2-ylethynyl)benzene) ligands (**2a–g**) (●).

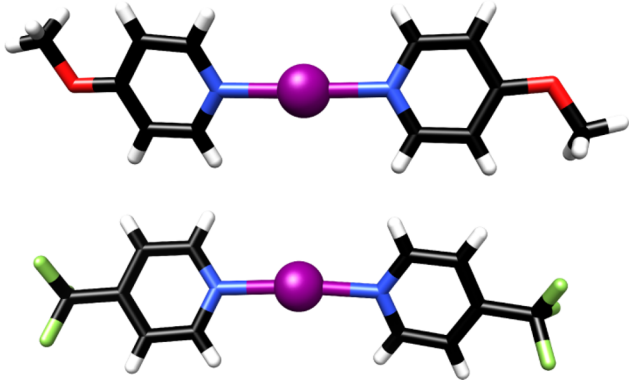

Figure 5. Solid state geometries of complexes **1c** (top, CCDC-1452897), and **1f** (bottom, CCDC-1452897), obtained by single crystal X-ray crystallography. The BF_4^- counterion is omitted from the figure for clarity. The crystal of compound **1c** was obtained as a solvate, and thus each molecular unit contains one molecule dichloroethane. Both complexes possess coplanar pyridine rings and nearly centrosymmetric geometries.

over 2 days. Crystallographic data for **1a** and **1d** were taken from the literature.[91,92] The X-ray crystallographic analysis confirmed that the N–I–N angle is linear (Figure 5) and that the iodine-centered complexes are symmetric, even in the solid state (Table 5), independent of their electron density. The small difference between the N–I bond lengths within a complex, lower than <0.4%, is likely due to crystal packing forces, and does not reflect a real asymmetry. Supporting the DFT predictions above, the X-ray crystallographic data corroborate that alteration of the electron density of the pyridine nitrogen causes only very minor, <2%, change in the N–I bond length.

Halogen Bond Strength in Solution Established by UV–vis Kinetics. For experimental evaluation of the electron density dependence of the halogen bond strength of [N–I–N]$^+$ complexes, we have monitored the rate of disappearance of the UV absorbance of [bis(pyridine)iodine)]$^+$ upon iodonium transfer from complexes **1a,c,d,f** to 4-penten-1-ol, using a procedure described by Neverov and Brown.[39,93] The mechanistic details of halonium transfer from bis(pyridine)-type complexes to alkenes are well understood.[39,93–97] We have used pseudo-first-order conditions, with a large excess of olefin

Table 5. X-ray Crystallographically Determined N–I Bond Distances and N–I–N Bond Angles for 1a,c,d,f

structure	4-R	r(N–X)$_1$ (Å)	r(N–X)$_2$ (Å)	σ (N–X–N) (deg)
1a[91]	H	2.260(3)	2.260(3)	180.0
		2.259(3)	2.259(3)	180.0
		2.255(3)	2.260(3)	177.7(1)
1c	OMe	2.252(3)	2.262(3)	178.0(1)
1d[92,a]	NMe_2	2.232	2.239	179.4
		2.247	2.252	177.7
1f	CF_3	2.251(5)	2.272(5)	176.2(2)
		2.256(5)	2.271(5)	175.2(2)

[a]The counterion of **1d** is NO_3^- instead of BF_4^-. This does not influence the geometry of [bis(pyridine)iodine]$^+$ complexes.

DOI: 10.1021/jacs.6b03842
J. Am. Chem. Soc. 2016, 138, 9853–9863

(3.9−77 mM), and monitored the reaction proceeding in dry dichloroethane solution at 25 °C at the wavelength of maximum change (**1a,f**: 230 nm, **1c**, 257 nm, and **1d**, 300 nm). The reactions of **1a,c,d** were monitored using a Cary 100 UV−vis spectrophotometer, whereas an Applied Photophysics SX-17MV stopped-flow reaction analyzer was used for the fast reactions with **1f** (4-CF_3). The observed rate constants (k_{obs}) were obtained by NLLSQ fitting of the absorbance versus time traces for the disappearance of the iodine(I) complex to the standard exponential model:

$$A_t = A_\infty + (A_0 - A_\infty)e^{-k_{obs}t} \quad (3)$$

The saturation profile obtained when plotting k_{obs} of **1a,c,f** against the alkene concentration implies that the mechanism for the iodonium transfer is similar to that previously proposed for bromocyclization with 4-penten-1-ol.[39] Saturation was not reached in the corresponding experiment with the electron rich and slowly reacting **1d**, suggesting a different rate limiting step. However, in the lower alkene concentration range the k_{obs} versus [4-penten-1-ol] profile was linear permitting determination of the second-order rate constant (k_2), even for this reaction. The logarithm of the second-order rate constants (k_2 = 9.21 M^{-1} s^{-1} (**1a**, H), k_2 = 1.92 M^{-1} s^{-1} (**1c**, OCH_3), k_2 = 0.00195 M^{-1} s^{-1} (**1d**, $N(Me)_2$), and k_2 = 126.9 M^{-1} s^{-1} (**1f**, CF_3)), normalized to 1 mM concentration of added 4-substituted pyridine, as a function of the change of natural atomic population, Δn(N), is shown in Figure 6.

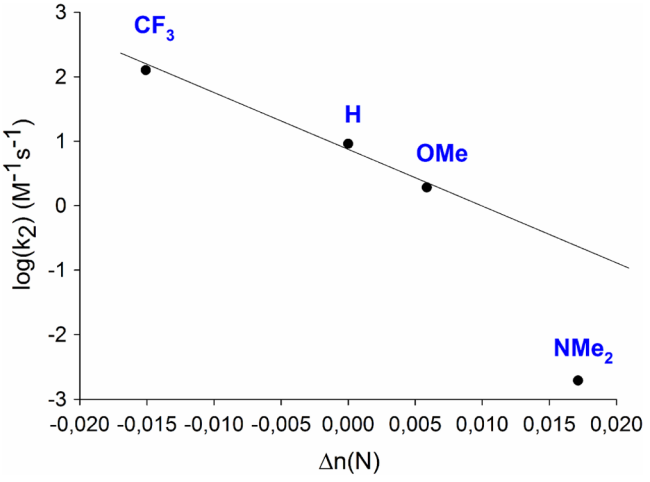

Figure 6. Second-order rate constants (M^{-1} s^{-1}) of **1a,c,d,f** in iodocyclization reactions with 4-penten-1-ol in the presence of 4-R-pyridine (R = H, OMe, NMe_2 or CF_3), normalized to 1 mM, obtained in dry dichloroethane, are shown as a function of the change of natural atomic population, Δn(N). A linear correlation is seen for all but the most electron rich complex **1d**.

The magnitude of the second-order rate constants of complexes **1a,c,d,f** follows the inverse order of substituent electronegativity, i.e., k_2(**1f**, CF_3) ≫ k_2(**1a**, H) > k_2(**1c**, OCH_3) ≫ k_2(**1d**, NMe_2). Whereas the log(k_2) of complexes **1a,c,f** correlates linearly to the change of natural atomic population, Δn(N), which corresponds to the Hammett σ_{para}, the corresponding log(k_2) of **1d** is an evident outlier (Figure 6), corroborating the hypothesis that the iodonium transfer mechanism for **1d** is different from that of its less electron rich analogues.

Due to the difficulties in identifying appropriate wavelengths for reaction monitoring, no kinetics experiments were undertaken for the analogous 4-substituted 1,2-bis((pyridine-2-ylethynyl)benzene)iodine(I) complexes **2a−f**.

We studied the kinetics of the dissociation of complexes **1a,c,e,f** in the presence of the strong XB acceptor 4-dimethylaminopyridine (DMAP), the free base of **1d**. This ligand exchange reaction is rapid due to the significantly higher stability of complex **1d** as compared to the less electron rich complexes. Moreover, the reaction is easy to follow as **1d** has high absorbance. The dissociation rate constants (k_{obs}) at 25 °C (Table 6) were determined from stopped-flow experiments by

Table 6. Dissociation of [Bis(4-R-pyridine)iodine]$^+$ Complexes 1a,c,f (7.68 × 10^{-5} M) in the Presence of an Excess DMAP (0.15 mM) in Dry Dichloroethane, Observed k_{obs} Dissociation Rate Constants at 298 K, and the Enthalpy and Entropy of Activation[a]

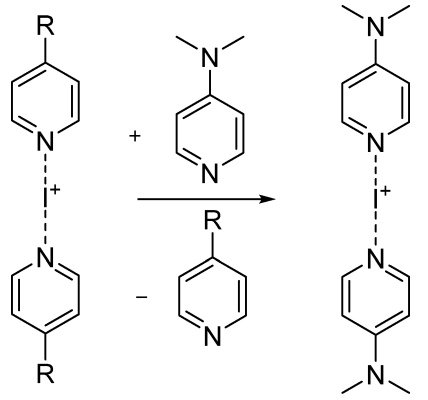

structure	4-R	k_{obs}[b] (s^{-1})	$\Delta H^{\ddagger}$[c] (kJ mol^{-1})	$\Delta S^{\ddagger}$[c] (J mol^{-1} K^{-1})
1a	H	0.392	70.97 ± 1.07	−14.45 ± 3.49
1c	OCH_3	0.333	72.83 ± 0.80	−13.23 ± 2.60
1f	CF_3	3.322	39.16 ± 1.87	−105.47 ± 6.15

[a]Experiments run under stopped-flow with 7.68 × 10^{-5} M iodine(I) complex **1a,c,f**, and 0.15 mM DMAP in the reaction cell. [b]Observed rate constants k_{obs} determined at 298 K. [c]Activation parameters, $\Delta H^{\ddagger}$ and $\Delta S^{\ddagger}$, determined from Eyring plots.

addition of DMAP (0.15 mM; concentration at which rate of the reaction was independent of [DMAP]) to **1a**, **1c**, or **1e** (7.68 × 10^{-5} M) in dry dichloroethane at 272 nm. We measured the initial rate kinetics for the formation of the DMAP coordinated complex **1d**. In addition, the thermodynamic activation parameters $\Delta H^{\ddagger}$ and $\Delta S^{\ddagger}$, shown in Table 6, for the reactions were determined from the same experiments performed at different temperatures (Table 6) by Eyring plots of the obtained k_{obs} rate constants. The obtained activation parameters indicate that the lower the electron density of an [N−I−N]$^+$ complex, the lower the activation barrier for iodine(I) transfer. This observation indicates, in excellent agreement with the DFT computations, that a decrease in electron density of the [N−I−N]$^+$ halogen bond decreases its strength.

■ CONCLUSIONS

Electron density changes do not disturb the symmetric geometry of the [N···I···N]$^+$ halogen bond of bis(pyridine)-type systems, neither in solution nor in the solid state. Despite having a strong influence on the strength of the halogen bond,

DOI: 10.1021/jacs.6b03842
J. Am. Chem. Soc. 2016, 138, 9853−9863

the electron density of the pyridine nitrogens does not significantly affect the N−I bond lengths. The slight change (<0.7%) correlates only weakly to the variation in total electron population, Δn(N), but much more strongly to that in the π population Δn(N). This observation is important to stress, as shortening of the halogen bond donor−acceptor distance is one of the most commonly used characteristics for categorizing halogen bond strength.

The ^{15}N NMR chemical shift of halogen bonded complexes is a good measure for the π electron population of the involved nitrogen. The ^{15}N NMR coordination shift of the studied iodine(I) complexes reflects the formation of the $[N{-}I{-}N]^+$ halogen bond; however, its magnitude does not directly reflect the strength of the halogen bond. Analogous lack of correlation between bond energy and chemical shift was recently reported for analogous tetrel bonds.[98]

The stability of the $[N{-}I{-}N]^+$ halogen bond correlates to the electron density of the nitrogen halogen bond acceptors. A linear correlation to the natural atomic population, Δn(N) of the *para*-substituted pyridines was seen for most substituents. However, reaction kinetics indicate that the iodine(I) complex bearing the strongly resonance donating *N*,*N*-dimethylamino substituent has a different iodonium transfer mechanism as compared to the other analogous complexes studied. Alkene halogenation using the latter 4-NMe_2-substituted complex is slow. On the whole, these observations may be helpful for providing a tool for thorough control of electrophilic halogenation reactions. As [bis(pyridine)iodine]$^+$ complexes are common synthetic reagents, this may be of significance for the development of new, stereoselective halogenating agents in the future.

■ ASSOCIATED CONTENT

Supporting Information

The Supporting Information is available free of charge on the ACS Publications website at DOI: 10.1021/jacs.6b03842.

Details on the synthesis, spectroscopic data for compound identification, and details on the NMR, computational, X-ray diffractometric, and kinetic investigations. (PDF)

■ AUTHOR INFORMATION

Corresponding Author

*mate@chem.gu.se

Present Addresses

[‖]Department of Biochemistry and Molecular Biology, Colorado State University, Fort Collins, Colorado 80523−1870, United States.

[▽]AstraZeneca, CVMD iMED, Pepparedsleden 1, Mölndal, 43183, Sweden.

[⊥]Department of Chemistry, Ångström Laboratory, Uppsala University, S-751 20 Uppsala, Sweden.

[¶]Chemtura Organometallics GmbH, Bergkamen, 59192 Germany.

[⊗]Afton Chemical, Richmond, Virginia 23219, United States.

Notes

The authors declare no competing financial interest.

■ ACKNOWLEDGMENTS

The research leading to these results has received funding from the European Research Council under the European Union's Seventh Framework Programme (FP7/2007-2013)/ERC Grant Agreement No. 259638. We thank the Swedish Research Council (ME 2007:4407; 621-2008-3562) and the Academy of Finland (KR: 263256 and 265328) for financial support, and Professor Stan Brown (Department of Chemistry, Queen's University) for giving us access to equipment for the UV−vis kinetic experiments.

■ REFERENCES

(1) Desiraju, G. R.; Ho, P. S.; Kloo, L.; Legon, A. C.; Marquardt, R.; Metrangolo, P.; Politzer, P.; Resnati, G.; Rissanen, K. *Pure Appl. Chem.* **2013**, *85*, 1711.

(2) Clark, T.; Hennemann, M.; Murray, J. S.; Politzer, P. *J. Mol. Model.* **2007**, *13*, 291.

(3) Huber, S. M.; Jimenez-Izal, E.; Ugalde, J. M.; Infante, I. *Chem. Commun.* **2012**, *48*, 7708.

(4) Kozuch, S.; Martin, J. M. *J. Chem. Theory Comput.* **2013**, *9*, 1918.

(5) Rezac, J.; Riley, K. E.; Hobza, P. *J. Chem. Theory Comput.* **2012**, *8*, 4285.

(6) Wang, C.; Danovich, D.; Mo, Y.; Shaik, S. *J. Chem. Theory Comput.* **2014**, *10*, 3726.

(7) Syzgantseva, O. A.; Tognetti, V.; Joubert, L. *J. Phys. Chem. A* **2013**, *117*, 8969.

(8) Wolters, L. P.; Bickelhaupt, F. M. *ChemistryOpen* **2012**, *1*, 96.

(9) Pinter, B.; Nagels, N.; Herrebout, W. A.; De Proft, F. *Chem. - Eur. J.* **2013**, *19*, 519.

(10) Cavallo, G.; Metrangolo, P.; Milani, R.; Pilati, T.; Priimagi, A.; Resnati, G.; Terraneo, G. *Chem. Rev.* **2016**, *116*, 2478.

(11) Ford, M. C.; Ho, S. P. *J. Med. Chem.* **2016**, *59*, 1655.

(12) Gilday, L. C.; Robinson, S. W.; Barendt, T. A.; Langton, M. J.; Mullaney, B. R.; Beer, P. D. *Chem. Rev.* **2015**, *115*, 7118.

(13) Berger, G.; Soubhye, J.; Meyer, F. *Polym. Chem.* **2015**, *6*, 3559.

(14) Catalano, L.; Cavallo, G.; Metrangolo, P.; Resnati, G.; Terraneo, G. *Top. Curr. Chem.* **2016**, *373*, 289.

(15) Mele, A.; Metrangolo, P.; Neukirch, H.; Pilati, T.; Resnati, G. *J. Am. Chem. Soc.* **2005**, *127*, 14972.

(16) Sarwar, M. G.; Dragisic, B.; Sagoo, S.; Taylor, M. S. *Angew. Chem., Int. Ed.* **2010**, *49*, 1674.

(17) Caballero, A.; White, N. G.; Beer, P. D. *Angew. Chem., Int. Ed.* **2011**, *50*, 1845.

(18) Zapata, F.; Caballero, A.; White, N. G.; Claridge, T. D.; Costa, P. J.; Felix, V.; Beer, P. D. *J. Am. Chem. Soc.* **2012**, *134*, 11533.

(19) Lim, J. Y.; Marques, I.; Ferreira, L.; Felix, V.; Beer, P. D. *Chem. Commun.* **2016**, *52*, 5527.

(20) Schindler, S.; Huber, S. M. *Top. Curr. Chem.* **2014**, *359*, 167.

(21) Wilcken, R.; Zimmermann, M. O.; Lange, A.; Joerger, A. C.; Boeckler, F. M. *J. Med. Chem.* **2013**, *56*, 1363.

(22) Yan, D.; Delori, A.; Lloyd, G. O.; Friscic, T.; Day, G. M.; Jones, W.; Lu, J.; Wei, M.; Evans, D. G.; Duan, X. *Angew. Chem., Int. Ed.* **2011**, *50*, 12483.

(23) Yan, D.; Bucar, D. K.; Delori, A.; Patel, B.; Lloyd, G. O.; Jones, W.; Duan, X. *Chem. - Eur. J.* **2013**, *19*, 8213.

(24) Bolton, O.; Lee, K.; Kim, H. J.; Lin, K. Y.; Kim, J. *Nat. Chem.* **2011**, *3*, 205.

(25) Priimagi, A.; Saccone, M.; Cavallo, G.; Shishido, A.; Pilati, T.; Metrangolo, P.; Resnati, G. *Adv. Mater.* **2012**, *24*, OP345.

(26) Yamamoto, H. M.; Kosaka, Y.; Maeda, R.; Yamaura, J.; Nakao, A.; Nakamura, T.; Kato, R. *ACS Nano* **2008**, *2*, 143.

(27) Okitsu, T.; Yumitate, S.; Sato, K.; In, Y.; Wada, A. *Chem. - Eur. J.* **2013**, *19*, 4992.

(28) Barluenga, J. *Pure Appl. Chem.* **1999**, *71*, 1385.

(29) Barluenga, J.; Gonzalez, J. M.; Campos, P. J.; Asensio, G. *Angew. Chem., Int. Ed. Engl.* **1985**, *24*, 319.

(30) Barluenga, J.; Gonzalez-Bobes, F.; Murguia, M. C.; Ananthoju, S. R.; Gonzalez, J. M. *Chem. - Eur. J.* **2004**, *10*, 4206.

(31) Lown, J. W.; Joshua, A. V. *Can. J. Chem.* **1977**, *55*, 122.

(32) Simonot, B.; Rousseau, G. *J. Org. Chem.* **1994**, *59*, 5912.

(33) Brunel, Y.; Rousseau, G. *Tetrahedron Lett.* **1995**, *36*, 8217.

(34) Brunel, Y.; Rousseau, G. *Tetrahedron Lett.* **1995**, *36*, 2619.

DOI: 10.1021/jacs.6b03842
J. Am. Chem. Soc. 2016, 138, 9853−9863

(35) Homsi, F.; Rousseau, G. *J. Org. Chem.* **1999**, *64*, 81.
(36) Rousseau, G.; Robin, S. *Tetrahedron Lett.* **1997**, *38*, 2467.
(37) Rousseau, G.; Robin, S. *Tetrahedron Lett.* **2000**, *41*, 8881.
(38) Andre, V.; Lahrache, H.; Robin, S.; Rousseau, G. *Tetrahedron* **2007**, *63*, 10059.
(39) Neverov, A. A.; Brown, R. S. *J. Org. Chem.* **1998**, *63*, 5977.
(40) Barluenga, J.; Vazquez-Villa, H.; Ballesteros, A.; Gonzalez, J. M. *J. Am. Chem. Soc.* **2003**, *125*, 9028.
(41) Fujioka, H.; Nakahara, K.; Hirose, H.; Hirano, K.; Oki, T.; Kita, Y. *Chem. Commun.* **2011**, *47*, 1060.
(42) Hakkert, S. B.; Erdelyi, M. *J. Phys. Org. Chem.* **2015**, *28*, 226.
(43) Carlsson, A.-C. C.; Veiga, A. X.; Erdelyi, M. *Top. Curr. Chem.* **2014**, *359*, 49.
(44) Carlsson, A.-C. C.; Grafenstein, J.; Laurila, J. L.; Bergquist, J.; Erdelyi, M. *Chem. Commun.* **2012**, *48*, 1458.
(45) Carlsson, A.-C. C.; Grafenstein, J.; Budnjo, A.; Laurila, J. L.; Bergquist, J.; Karim, A.; Kleinmaier, R.; Brath, U.; Erdelyi, M. *J. Am. Chem. Soc.* **2012**, *134*, 5706.
(46) Perrin, C. L. *Pure Appl. Chem.* **2009**, *81*, 571.
(47) Rissanen, K.; Haukka, M. *Top. Curr. Chem.* **2015**, *359*, 77.
(48) Metrangolo, P.; Neukirch, H.; Pilati, T.; Resnati, G. *Acc. Chem. Res.* **2005**, *38*, 386.
(49) Carlsson, A.-C. C.; Uhrbom, M.; Karim, A.; Brath, U.; Grafenstein, J.; Erdelyi, M. *CrystEngComm* **2013**, *15*, 3087.
(50) Bedin, M.; Karim, A.; Reitti, M.; Carlsson, A.-C. C.; Topic, F.; Cetina, M.; Pan, F. F.; Havel, V.; Al-Ameri, F.; Sindelar, V.; Rissanen, K.; Grafenstein, J.; Erdelyi, M. *Chem. Sci.* **2015**, *6*, 3746.
(51) Karim, A.; Reitti, M.; Carlsson, A.-C. C.; Grafenstein, J.; Erdelyi, M. *Chem. Sci.* **2014**, *5*, 3226.
(52) Haque, I.; Wood, J. L. *J. Phys. Chem.* **1968**, *72*, 2438.
(53) Erdelyi, M.; Gogoll, A. *J. Org. Chem.* **2001**, *66*, 4165.
(54) Kleinmaier, R.; Arenz, S.; Karim, A.; Carlsson, A.-C. C.; Erdelyi, M. *Magn. Reson. Chem.* **2013**, *51*, 46.
(55) Bechamp, A. *Annal. Chim. Phys.* **1854**, *42*, 186.
(56) Hamilton, C. S.; Morgan, J. F. *Org. React.* **1944**, *2*, 428.
(57) Heemstra, J. M.; Moore, J. S. *Org. Lett.* **2004**, *6*, 659.
(58) Cai, D. W.; Hughes, D. L.; Verhoeven, T. R. *Tetrahedron Lett.* **1996**, *37*, 2537.
(59) Wolfe, S.; Yang, K.; Weinberg, N.; Shi, Z.; Hsieh, Y. H.; Sharma, R. D.; Ro, S.; Kim, C. K. *Chem. - Eur. J.* **1998**, *4*, 886.
(60) Rigel Pharmaceuticals INC, WO 2004/018463 A2, 2004 INC, R. P.; Organization, W. I. P., Ed. 2004.
(61) Sagitullina, G. P.; Vorontsova, M. A.; Garkushenko, A. K.; Poendaev, N. V.; Sagitullin, R. S. *Russ. J. Org. Chem.* **2010**, *46*, 1830.
(62) Dumele, O.; Wu, D.; Trapp, N.; Goroff, N.; Diederich, F. *Org. Lett.* **2014**, *16*, 4722.
(63) Khavasi, H. R.; Hosseini, M.; Tehrani, A. A.; Naderi, S. *CrystEngComm* **2014**, *16*, 4546.
(64) Troff, R. W.; Makela, T.; Topic, F.; Valkonen, A.; Raatikainen, K.; Rissanen, K. *Eur. J. Org. Chem.* **2013**, *2013*, 1617.
(65) Geer, M. F.; Mazzuca, J.; Smith, M. D.; Shimizu, L. S. *CrystEngComm* **2013**, *15*, 9923.
(66) Solimannejad, M.; Malekani, M.; Alkorta, I. *J. Phys. Chem. A* **2013**, *117*, 5551.
(67) Bauza, A.; Quinonero, D.; Frontera, A.; Deya, P. M. *Phys. Chem. Chem. Phys.* **2011**, *13*, 20371.
(68) Reed, A. E.; Weinstock, R. B.; Weinhold, F. *J. Chem. Phys.* **1985**, *83*, 735.
(69) Andersson, H.; Carlsson, A.-C. C.; Nekoueishahraki, B.; Brath, U.; Erdelyi, M. *Annu. Rep. NMR Spectrosc.* **2015**, *86*, 73.
(70) Castro-Fernandez, S.; Lahoz, I. R.; Llamas-Saiz, A. L.; Alonso-Gomez, J. L.; Cid, M. M.; Navarro-Vazquez, A. *Org. Lett.* **2014**, *16*, 1136.
(71) Puttreddy, R.; Jurcek, O.; Bhowmik, S.; Makela, T.; Rissanen, K. *Chem. Commun.* **2016**, *52*, 2338.
(72) Holtz, D. *Chem. Rev.* **1971**, *71*, 139.
(73) Saunders, M.; Telkowski, L.; Kates, M. R. *J. Am. Chem. Soc.* **1977**, *99*, 8070.
(74) Siehl, H. U. *Adv. Phys. Org. Chem.* **1987**, *23*, 63.
(75) van't Hoff, J. H. Z. *Z. Phys. Chem.* **1887**, *1*, 783.
(76) Perrin, C. L.; Karri, P. *J. Am. Chem. Soc.* **2010**, *132*, 12145.
(77) Becke, A. D. *J. Chem. Phys.* **1993**, *98*, 5648.
(78) Lee, C.; Yang, W.; Parr, R. G. *Phys. Rev. B: Condens. Matter Mater. Phys.* **1988**, *37*, 785.
(79) Vosko, S. H.; Wilk, L.; Nusair, M. *Can. J. Phys.* **1980**, *58*, 1200.
(80) Roy, L. E.; Hay, P. J.; Martin, R. L. *J. Chem. Theory Comput.* **2008**, *4*, 1029.
(81) Hay, P. J.; Wadt, W. R. *J. Chem. Phys.* **1985**, *82*, 270.
(82) Hay, P. J.; Wadt, W. R. *J. Chem. Phys.* **1985**, *82*, 299.
(83) Hay, P. J.; Wadt, W. R. *J. Chem. Phys.* **1985**, *82*, 284.
(84) Clark, T.; Chandrasekhar, J.; Spitznagel, G. W.; Schleyer, P. V. *J. Comput. Chem.* **1983**, *4*, 294.
(85) Francl, M. M.; Pietro, W. J.; Hehre, W. J.; Binkley, J. S.; Gordon, M. S.; Defrees, D. J.; Pople, J. A. *J. Chem. Phys.* **1982**, 77.
(86) Krishnan, R.; Binkley, J. S.; Seeger, R.; Pople, J. A. *J. Chem. Phys.* **1980**, *72*, 650.
(87) Cossi, M.; Scalmani, G.; Rega, N.; Barone, V. *J. Chem. Phys.* **2002**, *117*, 43.
(88) Mennucci, B.; Tomasi, J. *J. Chem. Phys.* **1997**, *106*, 5151.
(89) Lommerse, J. P. M.; Stone, A. J.; Taylor, R.; Allen, F. H. *J. Am. Chem. Soc.* **1996**, *118*, 3108.
(90) Ebrahimi, A.; Razmazma, H.; Delarami, H. S. *Phys. Chem. Res.* **2016**, *4*, 1.
(91) Alvarez-Rua, C.; Garcia-Granda, S.; Ballesteros, A.; Gonzalez-Bobes, F.; Gonzalez, J. M. *Acta Crystallogr., Sect. E: Struct. Rep. Online* **2002**, *58*, O1381.
(92) Georgiou, D. C.; Butler, P.; Browne, E. C.; Wilson, D. J. D.; Dutton, J. L. *Aust. J. Chem.* **2013**, *66*, 1179.
(93) Neverov, A. A.; Feng, H. X. M.; Hamilton, K.; Brown, R. S. *J. Org. Chem.* **2003**, *68*, 3802.
(94) Brown, R. S.; Nagorski, R. W.; Bennet, A. J.; Mcclung, R. E. D.; Aarts, G. H. M.; Klobukowski, M.; Mcdonald, R.; Santarsiero, B. D. *J. Am. Chem. Soc.* **1994**, *116*, 2448.
(95) Neverov, A. A.; Muise, T. L.; Brown, R. S. *Can. J. Chem.* **1997**, *75*, 1844.
(96) Neverov, A. A.; Brown, R. S. *J. Org. Chem.* **1996**, *61*, 962.
(97) Cui, X. L.; Brown, R. S. *J. Org. Chem.* **2000**, *65*, 5653.
(98) Southern, S. A.; Bryce, D. L. *J. Phys. Chem. A* **2015**, *119*, 11891.

DOI: 10.1021/jacs.6b03842
J. Am. Chem. Soc. 2016, 138, 9853−9863